Progress Towards the Synthesis of Succinate-derived Flexible Peptide for the Src SH2 Domain

Presented by: Vincent Au

In partial fulfillment of the requirements for graduation with the
Dean's Scholars Honor's Degree in Biochemistry

Supervising Professor

_____ _____
Dr. Stephen F. Martin Date

Honors Advisor in Chemistry/Biochemistry

_____ _____
Dr. John F. Stanton Date

Progress Towards the Synthesis of Succinate-derived Flexible Peptide for the Src SH2 Domain

I grant the Dean's Scholars Program permission to:
____X____ Post a copy of my thesis on the Dean's Scholars website
____X____ Keep a copy of my thesis in the Dean's Scholars Office

_____
Vincent Au

_____
Signature Date

_____
Dr. Stephen F. Martin

_____
Signature Date

Abstract

Preorganizing a flexible ligand in the shape it adopts when bound to a protein should theoretically result in an increased binding affinity due to a smaller entropic penalty during binding. Previous work, however, shows that this is not always the case. Constraining the pY residue of a short peptidic sequence, pYEEI, that binds to the Src Homology 2 domain of the Src kinase (Src SH2 domain) resulted in an entropic advantage, but this was offset by an enthalpic penalty that resulted in approximately equal binding affinities of the flexible and constrained ligands. Based on NMR relaxation and molecular dynamics studies of the complex, it is hypothesized that suboptimal interactions within the pY binding site ("binding hot spot") may be the reason for the loss of enthalpy. In order to test this hypothesis, a cyclopropane-derived replacement for the isoleucine residue, which binds to a hydrophobic site of the domain, and its succinate-derived flexible analog are being synthesized. This paper reports the synthesis progress towards the flexible analog.

Introduction

All biological processes depend on specific recognition between molecules. In cell signal transduction, for example, a hormonal ligand first interacts with an intracellular or cell-surface receptor that induces a cascade of downstream signals which involve protein-protein, protein-ligand, and protein-nucleic acid interactions that ultimately leads to a cellular response. Given its universal nature, disrupting protein-protein interactions is an important strategy in medicinal chemistry. However, current understanding of the physical basis behind these interactions is still limited. It is very difficult, and sometimes impossible, to predict binding affinities even when high-resolution structural data is available. Structure-based drug design has been limited in this sense, but understanding how structure relates to binding affinity remains vitally important as this knowledge may ultimately aid in the more efficient designs of novel drugs.

Predicting binding affinity is a complex problem due to multiple contributing thermodynamic processes.[1,2] A protein-ligand interaction can be described as an equilibrium between the bound and unbound states and is written in the form:

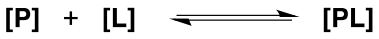

The association constant K_a is related to the relative concentrations of the protein-ligand complex (PL) and the free protein (p) and ligand (l) in solution through equation 1.

$$K_a = \frac{[PL]}{[P][L]} \quad (1)$$

Conversely, the dissociation constant K_d is the reciprocal of K_a and is used in biochemistry and pharmacology to report the molar concentration of ligand at which half of the available ligand-binding sites are occupied. A large K_a value, or small K_d value, indicates strong complexation

between protein and ligand to form the protein-ligand complex. The change in standard Gibbs' free energy of binding (ΔG_b^o) is a function of the equilibrium constant K_a (equation 2).

$$\Delta G_b^o = -RT \ln K_a \quad (2)$$

Note that this is the standard energy of binding and not the free energy of binding ΔG_b, which is zero at equilibrium by definition. ΔG_b^o is also related to change in enthalpy (ΔH) and change in entropy (ΔS) through the Gibbs' free energy relationship (equation 3).

$$\Delta G_b^o = \Delta H_b^o - T\,\Delta S_b^o \quad (3)$$

To design a ligand with high binding affinity, both ΔH^o_b and ΔS^o_b must be optimized to give a negative value for ΔG^o_b (i.e. a large positive K_a value). One way this could be accomplished is by altering the structure of the ligand to maximize favorable structural interactions between protein and ligand. However, the process is not as easy as fitting a lock and key.

As described, two thermodynamic parameters contribute to the overall binding affinity: enthalpy and entropy. For the simple model presented above, ignoring any solvent effects, the binding enthalpy can be loosely defined as the static, structural component of the interaction between protein and ligand. A favorable change in enthalpy is commonly attributed to effective noncovalent interactions such as hydrogen bonding and van der Waals forces between the protein and ligand. On the other hand, entropy (S) is the measure of disorder of a system. For the protein-ligand system, it refers to the vibrational, translational, rotational, and internal rotational freedom of the protein and ligand. The change in entropy is loosely related to the dynamics of the system and depends on the change in dynamics of the protein-ligand complex and of the individual partners before association.

In reality, protein-ligand interactions are more complicated than the bimolecular model presented above. In addition to the structure and dynamics of protein and ligand, one must also account for the solvent (water) which has a large effect on binding. A modified representation of protein-ligand interactions is shown in the Borne-Haber Cycle (Figure 1).[1]

Figure 1

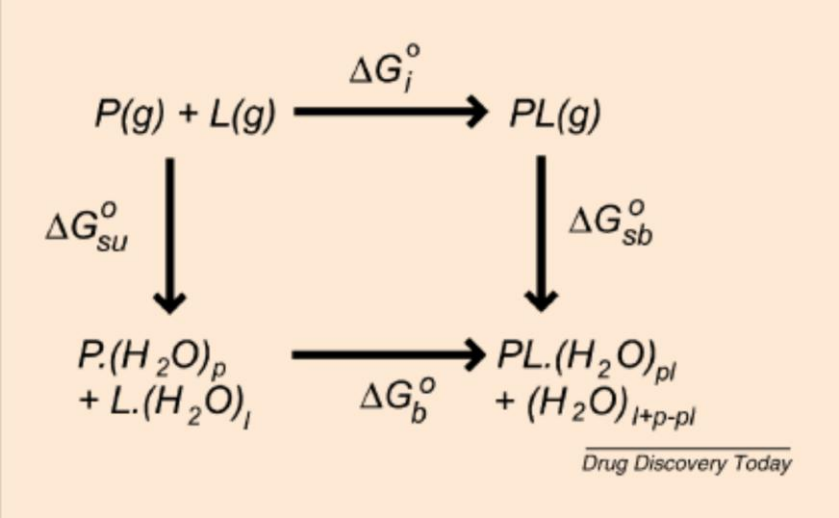

Homans, S.W. *Drug Discovery Today*. **2007**, *12*, 534-539.

Here, ΔG_b^o takes into account the complex's interaction with water and represents the observed standard Gibbs' free energy of binding. ΔG_i^o is the 'intrinsic' free energy of binding and represents the protein and ligand interaction in the absence of water. ΔG_{su}^o and ΔG_{sb}^o equates to the solvation energy of the free species and the complex respectively. Since ΔG_b^o comprisesΔH_b^o and ΔS_b^o, one can also break down the observed ΔH_b^o and ΔS_b^o into parts as illustrated above.

One strategy in structure-based ligand design is constraining the ligand (such as peptides and other small molecules) in its biologically active, or "bound," form in order to improve

binding affinity.[3] The reasoning behind this approach is that a preorganized ligand will have a lower entropic penalty paid upon binding. To elaborate, when a ligand and a protein form a complex, the theoretical change in entropy for the ligand is negative (or unfavorable) since the ligand loses rotational degrees of freedom upon binding. By restricting the initial conformational freedom of the ligand, this negative change in entropy should be reduced which would result in a higher overall binding affinity.

Previous work with preorganization in the Martin lab involves the Src homology 2 (SH2) domain of the growth factor receptor-bound protein 2 (Grb2) and of Src tyrosine kinase (Src).[4,5] The SH2 domain binds proteins containing phosphorylated tyrosine residue (abbreviated pY) and is important in various signal transduction pathways. Inhibitors of this domain have been extensively studied with the aim of targeting the Ras pathway and osteoclastic bone resorption (for Grb2 and Src respectively).[6,7] Structural and thermodynamic studies of peptide analogs to the SH2 domain of both proteins show that the general assumption that preorganizing a flexible ligand will result in a more favorable binding affinity due to a lower entropic penalty does not always hold true. In Grb2 SH2, for example, although the constrained ligand **(1)** binds approximately two-fold better than the flexible counterpart **(2)**, it bound with a less favorable change in entropy.[4]

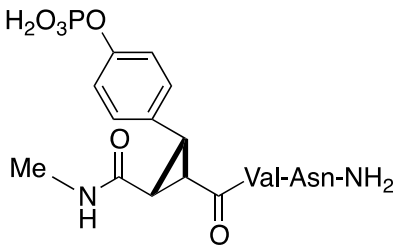

1

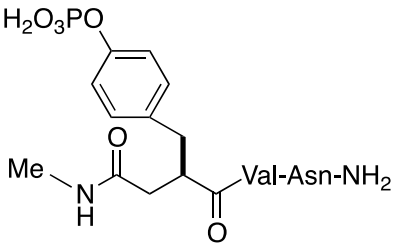

2

For Src SH2, the pY-constrained ligand **(3)** bound with more favorable entropy than the flexible mimic **(4)** as expected. However, this was offset by an enthalpic penalty which resulted in approximately equal binding affinities of the flexible and constrained ligands (ref.). There was a minimal improvement in binding affinity for both constrained and flexible analogs compared to the known antagonist **pYEEI** (Table 1).[5]

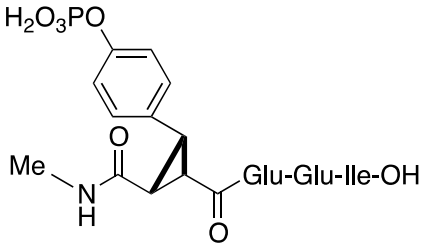

3

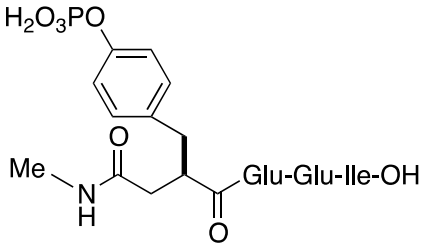

4

Table 1

Peptide	K_a	ΔG (kcal/mol)	ΔH (kcal/mol)	ΔS (cal/mol K)
Ac-pYEEI	$4.1(\pm 0.1)*10^6$	-9.01 ± 0.01	-6.06 ± 0.05	9.9 ± 0.2
3	$1.0(\pm 0.1)*10^7$	-9.55 ± 0.07	-5.91 ± 0.04	17 ± 1
4	$1.7(\pm 0.6)*10^7$	-9.8 ± 0.2	-7.33 ± 0.03	8.3 ± 0.5

The physical basis of these thermodynamic values could not be explained from crystal structure data alone. However, follow-up NMR spectroscopy and molecular dynamics stimulations studies of the protein complexes reveal that the conformational constraints on the pY residue alter the geometry of important polar contacts in the binding pocket.[8] This suggests that suboptimal interactions in this "binding hot spot" may be the reason for the loss of enthalpy.

To test this hypothesis, a cyclopropane-derived replacement for the isoleucine residue **(5)** and its succinate-derived flexible analog **(6)** are being synthesized.

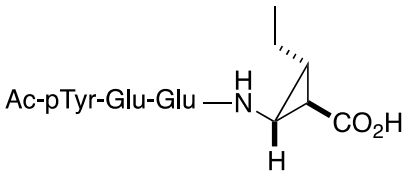

5

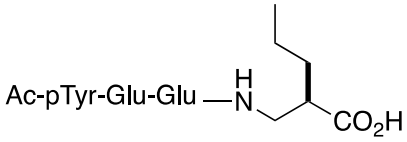

6

Specific Aim

To further probe the effect of ligand preorganization in Src SH2 domain, the flexible mimic **6** is being synthesized. The binding thermodynamics of this compound will later be determined by isothermal titration calorimetry. Furthermore, the crystal structure of the protein-ligand complex will be analyzed and possibly follow-up NMR relaxation and molecular dynamics studies will be performed.

Results and Discussion

The synthesis of the succinate-derived flexible peptide mimic **6** was designed by Dr. Tian, and is based upon previous methods used by the Martin lab.[9] **Scheme 1** shows the retrosynthetic analysis. The synthesis of the peptide was envisioned from the coupling of β-amino ester **7** and amino acid derivatives. The β-amino ester would be synthesized via a Curtius rearrangement of acid **8** followed by cleavage of the auxiliary. The acid would be synthesized by alkylating the chiral imide **9** with benzyl 2-bromoacetate followed by hydrogenolysis of the benzyl ester using H_2 in the presence of a Pd/C catalyst.

Scheme 1

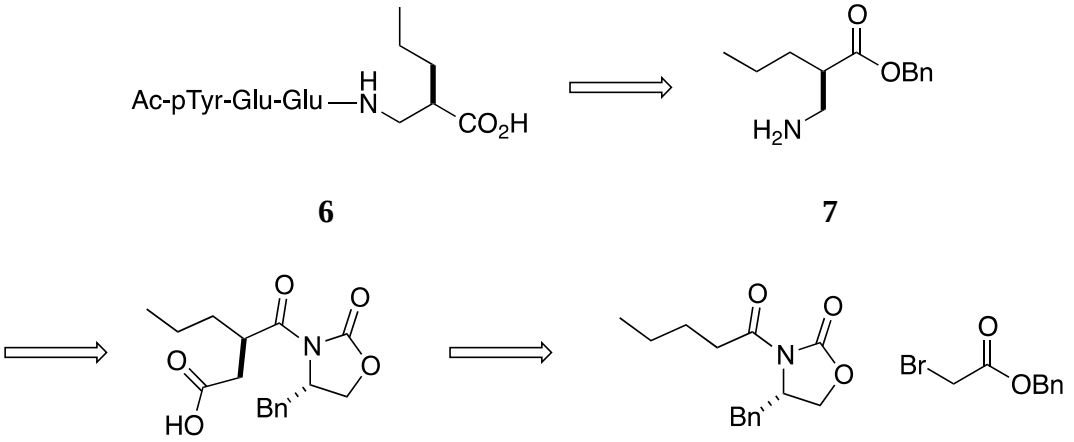

To synthesize the auxiliary, L-phenylalanine **10** was first reduced to L-phenylalaninol **11 (Scheme 2)** using borane, which was generated *in situ* from $NaBH_4$ in an 85% yield, similar to literature values.[10]

Scheme 2

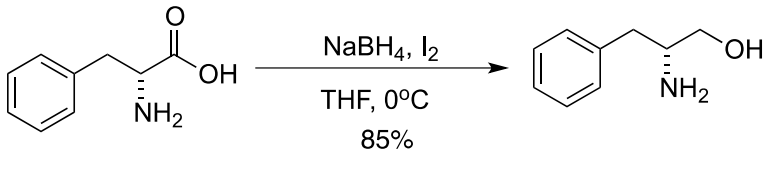

The alcohol is treated with diethyl carbonate and K_2CO_3 **(Scheme 3)** under reflux to form the Evan's auxiliary **12**.[11] Initially, a mixed solution of hexanes and ethyl acetate (2:1) was used to recrystallize, but it did not work. The impure auxiliary was therefore purified by column chromatography and then recrystallized from a solution of toluene and hexanes (1:1). This may be the reason for a low yield (25%).

Scheme 3

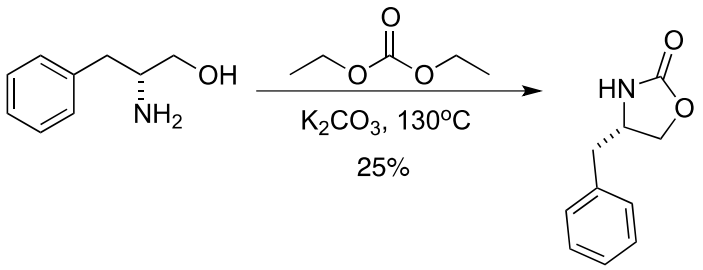

11 **12**

The auxiliary is then coupled to valeric acid **(Scheme 4)**. The acid is first deprotonated using triethylamine and reacts with pivaloyl chloride to form the mixed anhydride at -15°C. Then the auxiliary is added along with lithium chloride to the solution. Lithium chloride acts as a lewis acid and coordinates to the carbonyl oxygen of the auxiliary which makes the proton on the nitrogen more acidic allowing deprotonation by triethylamine. The auxiliary is allowed to react with the mixed anhydride under room temperature overnight and yields the chiral imide **9** (80%). This mechanism is notable: in the first reaction run, lithium chloride was not added into the reaction flask before letting the mixture stir overnight. This mistake was spotted the next day, and lithium chloride was added before letting the reaction run again overnight. However, the reaction did not progress after adding lithium chloride the next day.

Scheme 4

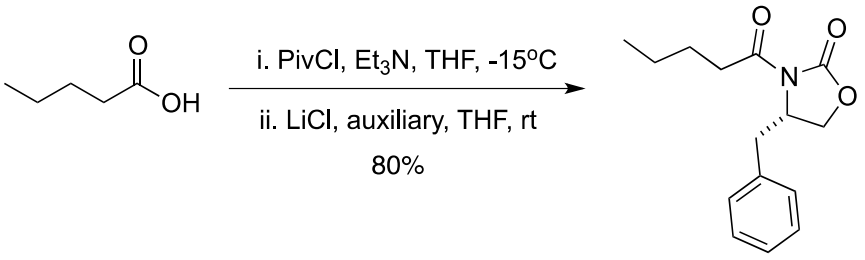

9

The chiral imide is treated with sodium bis(trimethylsilyl)amide (NaHMDS) at -78^{o}C for 1 hour to deprotonate the alpha carbon and form the enolate. Afterwards, benzyl 2-bromoacetate was added dropwise to the solution and allowed to stir for 3 hours. Asymmetric alkylation to form **13** was achieved by chelation of the enolate complex by sodium from NaHMDS. Dr. Tian previously reported a 70% yield for this reaction. However, this paper reports only a 34% yield. One reason for the lower yield is difficulty in purification. Mixed fractions were identified, but they have not been further purified.

Scheme 5

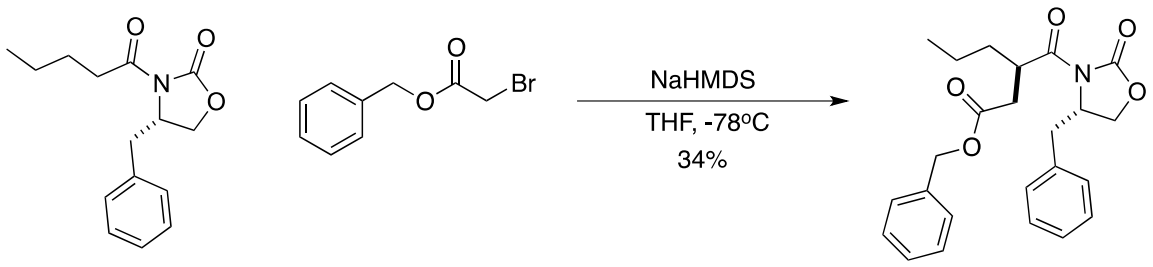

9 **13**

The acid (**8**) was formed from **13** by a hydrogenolysis reaction using palladium on carbon catalyst under H_2 **(Scheme 6)**. The reaction went to completion in less than 2 hours as opposed to overnight as previously reported. The resulting mixture was filtered through a celite plug using ethanol and concentrated to yield a colorless, soapy oil, in a near quantitative yield (98%).

Scheme 6

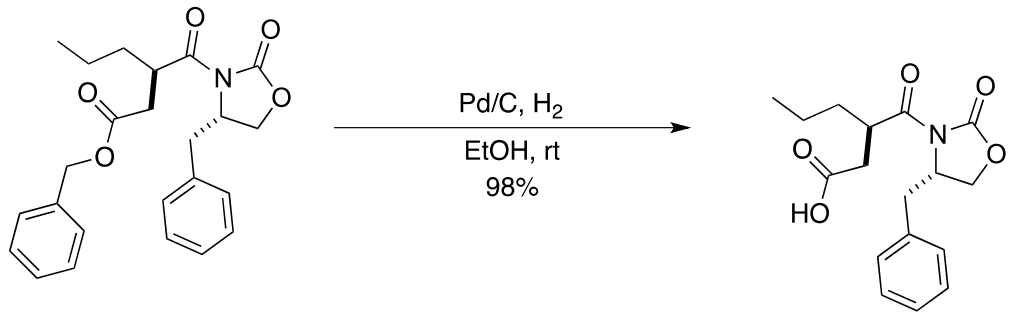

13 **8**

Dr. Tian previously treated the acid with diphenylphosphoryl azide (DPPA) and triethyl amine to form the isocyanate via a Curtius rearrangement. This was then reacted with *tert*-butanol to form the carbamate **14 (Scheme 7)**. However, he reported a low yield (32%) with the major product being a urea. This reaction was performed with the same procedure, and the yield was similar (28%).

Scheme 7

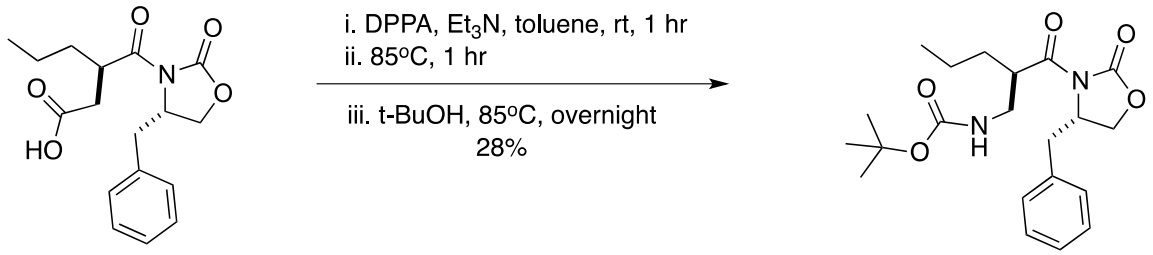

8 **14**

The last step of this reaction involves displacing the auxiliary on the carbamate with benzyl alcohol **(Scheme 8)**. This reaction was performed by Dr. Tian with a yield of 62%.

Scheme 8

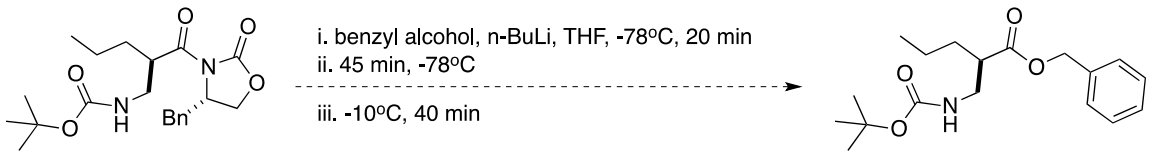

14 **15**

An alternative approach was sought to improve the yield for the Curtius rearrangement. We believe that the benzyl group sterically hinders the addition of the azide to the acid and the subsequent attack by *tert*-butanol. To avoid this problem, the sequence of the last two steps was switched: the auxiliary was first displaced by benzyl alcohol to form **16 (Scheme 9)** followed by the Curtius rearrangement to form **7 (Scheme 10)**. This sequence also avoids having to protect the amine with *tert*-butanol. The reaction in **Scheme 9** has been performed and the product has been identified using LC-MS. However, it still needs to be purified (hence no yield).

Scheme 9

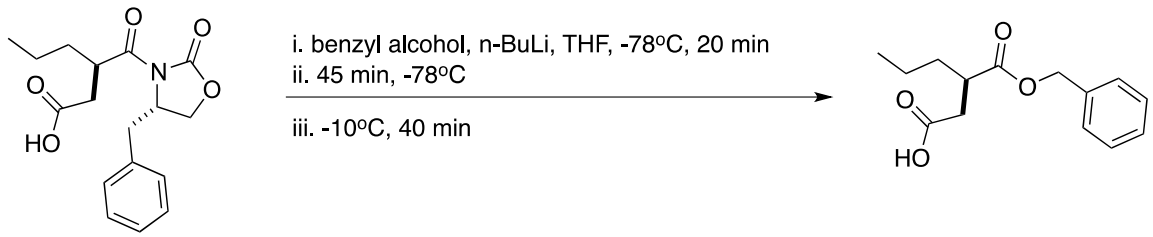

8 **16**

Scheme 10

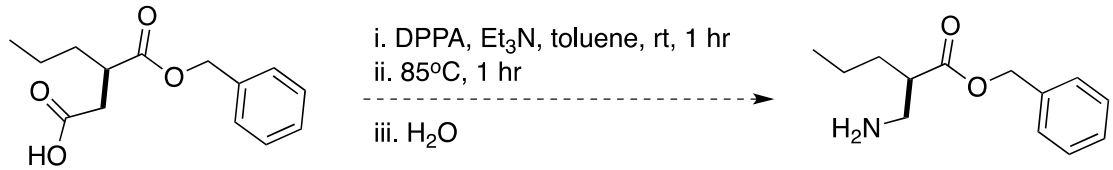

16 **7**

Conclusion

The primary purpose of this project is to synthesize the succinate-derived flexible peptide **6** to study its binding thermodynamics. Currently, attempts are being made to synthesize the amino acid **7** using a modified method to the one initially developed by Dr. Tian. Several key intermediates including the acid **(8)**, the imide **(9)**, and Evan's auxiliary **(12)** have been synthesized with a high yield and are available for any needed future reactions. However, the current immediate goal is to purify and characterize the new compound **15**. Once this reaction is optimized, it will be scaled up and the last step **(Scheme 10)** will be attempted to create amino acid **7**.

Experimental section

General. Tetrahydrofuran and diethyl ether were dried by filtration through two columns of activated, neutral alumina according to the procedure described by Grubbs.[12] Methanol (MeOH), acetonitrile (MeCN), and dimethylformamide (DMF) were dried by filtration through two columns of activated molecular sieves, and toluene was dried by filtration through one column of activated, neutral alumina followed by one column of Q5 reactant. These solvents were determined to have less than 50 ppm H_2O by Karl Fischer coulometric moisture analysis. Benzene, methylene chloride (CH_2Cl_2), diisopropylamine (*i*-Pr_2NH), triethylamine (Et_3N), diisopropylethylamine (*i*-Pr_2Net), and pyridine were distilled from calcium hydride immediately prior to use. All reagents were reagent grade and used without purification unless otherwise noted, and air or moisture sensitive reagents were weighed in a glove box. All reactions involving air or moisture sensitive reagents or intermediates were performed under an inert atmosphere of nitrogen or argon in glassware that was flame or oven dried. Solutions were degassed using three freeze-pump-thaw cycles under vacuum. Reaction temperatures refer to the temperature of the cooling/heating bath. Volatile solvents were removed under reduced pressure

using a Büchi rotary evaporator at 25–30 °C (bath temperature). Thin layer chromatography was run on pre-coated plates of silica gel with a 0.25 mm thickness containing 60F-254 indicator (EMD Millipore). Chromatography was performed using forced flow (flash chromatography) and the indicated solvent system on 230-400 mesh silica gel (Silicycle flash F60) according to the method of Still,[13] unless otherwise noted.

Infrared (IR) spectra were obtained either neat on sodium chloride or as solutions in the solvent indicated and reported as wavenumbers (cm^{-1}). Proton nuclear magnetic resonance (^{1}H NMR) and carbon nuclear magnetic resonance (^{13}C NMR) spectra were obtained at the indicated field as solutions in $CDCl_3$ unless otherwise indicated. Chemical shifts are referenced to the deuterated solvent (*e.g.,* for $CDCl_3$, δ = 7.26 ppm and 77.0 ppm for ^{1}H and ^{13}C NMR, respectively) and are reported in parts per million (ppm, δ) relative to tetramethylsilane (TMS, δ = 0.00 ppm). Coupling constants (*J*) are reported in Hz and the splitting abbreviations used are: s, singlet; d, doublet; t, triplet; q, quartet; m, multiplet; comp, overlapping multiplets of magnetically nonequivalent protons; br, broad; app, apparent.

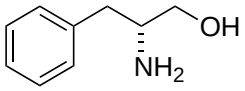

11

(R)-2-Amino-3-phenylpropan-1-ol (11). (VA-41) $NaBH_4$ (6.92 g, 183 mmol) was dissolved in THF (200 mL) under an atmosphere of Ar at 0 ºC. L-Phenylalanine (12.55 g, 76 mmol) was then added in one portion. To this mixture was added I_2 (19.30 g, 76 mmol) in THF (50 mL) via a syringe pump over a period of 1 h, resulting in a vigorous evolution of H_2. After addition of I_2 and evolution of H_2 had ceased, the vessel was heated under reflux for 18 h and then cooled to room temperature. Methanol was cautiously added until the mixture was clear.

The resulting colorless solution was concentrated under reduced pressure to give a white, sticky paste, which was dissolved by stirring overnight in 20% KOH (150 mL). The solution was extracted with CH_2Cl_2 (4 x 150 mL), dried (Na_2SO_4), and concentrated to afford a white solid that was recrystallized from toluene to yield 9.754 g (85%) of **11** as white needles: mp 92-94 ^oC.

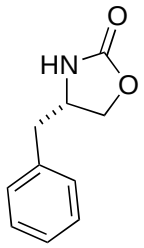

12

(S)-4-Benzyloxazolidin-2-one (12). (VA-49) Phenylalaninol (10.53 g, 69.6 mmol), diethyl carbonate (16.03 g, 16.44 mL, 142.76 mmol), and anhydrous potassium carbonate (0.962 g, 6.96 mmol) was stirred at 130 ^oC for 4 h, with removal of ethanol by distillation. After cooling to room temperature, it was extracted with EtOAc (325 mL), washed with 1 M HCl (25 mL), dried (Mg_2SO_4), and concentrated under reduced pressure. The sample was recrystallized from a mixed solvent of hexanes:toluene (1:1) to yield 3.1 g (25%) of **12** as a colorless solid: mp 84-86 ^oC.

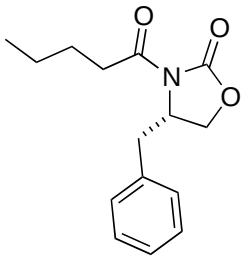

9

(S)-4-Benzyl-3-pentanoyloxazolidin-2-one (9). (VA-73) Valeric acid (1.56 g, 1.68 mL, 15.25 mmol) and Et_3N (2.98 g, 4.11 mL, 29.45 mmol) was dissolved in THF (26 mL) in a round-bottom flask under nitrogen and cooled to -10 ^oC. Pivaloyl chloride (2.2 g, 2.25 mL, 18.29 mmol) was added dropwise to this solution, and the mixture was allowed to stir for 2.5 h. Lithium chloride (0.78 g, 18.3 mmol) was added to this solution. Then the oxazolidinone (3.241 g, 18.29 mmol) dissolved in THF (39 mL) was added dropwise to the mixture. The cooling bath was removed and the mixture was stirred at rt for 14 h. EtOAc (125 mL) was added and the mixture was washed with saturated $NaHCO_3$ (40 mL). The organic layer was washed with brine (40 mL), dried (Mg_2SO_4), and concentrated under reduced pressure to give a yellow liquid. This was purified by flash chromatograph eluting with hexane/EtOAc (5:1) to give 3.159 g (80%) of **9** as a colorless oil: ^{1}HNMR (400 MHz, $CDCl_3$) δ 7.34 (m, 2 H), 7.28 (m, 1 H), 7.22 (m, 2 H), 4.68 (m, 1 H), 4.18 (m, 2 H), 3.30 (dd, J = 3.2, 13.6 Hz, 1 H), 2.95 (m, 2 H), 2.77 (dd, J = 9.6, 13.6 Hz, 1 H), 1.68 (m, 2 H), 1.42 (hex, J = 7.2 Hz, 2 H), 0.96 (t, J = 7.2 Hz, 3 H).

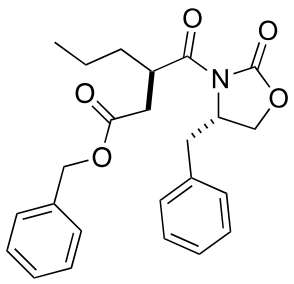

13

(*R*)-Benzyl 3-((*S*)-4-benzyl-2-oxooxazolidine-3-carbonyl)hexanoate (13). (VA-79) The imide **9** and benzyl 2-bromoacetate was dissolved in toluene and concentrated under reduced pressure. The imide (1.5 g, 5.74 mmol) was placed into a round-bottom flask, dissolved in THF (66 mL), and cooled to -78 ^oC. NaHMDS (0.443 M, 16.9 mL, 7.46 mmol) was added dropwise

to this solution. The mixture was stirred for 1 h. A solution of benzyl 2-bromoacetate (1.814 g, 7.92 mmol) dissolved in THF (33 mL) was added dropwise to this mixture. The resulting mixture was stirred for 2 h and quenched with saturated NH_4Cl (30 mL). The mixture was extracted with EtOAc (4 x 50 mL), and the combined organic layers were dried (Mg_2SO_4) and concentrated under reduced pressure. The crude product was purified using flash chromatography (elution gradient from 0% to 30% EtOAc in hexanes) to give 0.801 g (34%) of **13** as colorless oil: ^{1}HNMR (400 MHz, $CDCl_3$) δ 7.35-7.21 (comp, 10 H), 5.11 (s, 2 H), 4.62 (m, 1 H), 4.27 (m, 1 H), 4.12 (m, 2 H), 3.24 (dd, J = 2.8, 13.6 Hz, 1 H), 2.98 (dd, J = 11.2, 17.2 Hz, 1 H), 2.62 (dd, J = 4.4, 17.2 Hz, 1 H), 2.48 (dd, J = 10.4, 14.0 Hz, 1 H), 1.66 (m, 1 H), 1.52-1.32 (comp, 4 H), 0.92 (t, J = 7.2 Hz, 3 H).

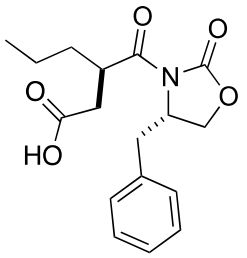

8

(*R*)-3-((*S*)-4-Benzyl-2-oxooxazolidine-3-carbonyl)hexanoic acid (8). (VA-67) Alkylated product **13** (92.2 mg, 0.225 mmol) was dissolved in EtOH (1.76 mL). The flask was purged three times with N_2, 10% Pd/C catalyst (23.9 mg) was added to the solution, and the flask was placed under H_2. The mixture was stirred for 2 h and then filtered through a celite plug which was washed with EtOH (3 mL) thoroughly. The filtrate was concentrated under reduced pressure to give 70 mg (98%) of **8** as a colorless foam: ^{1}HNMR (400 MHz, $CDCl_3$) δ 7.36-7.24 (comp, 5 H), 4.66 (m, 1 H), 4.23-4.16 (comp, 3 H), 3.28 (dd, J = 3.2, 13.6 Hz, 1 H), 2.95 (dd, J =

10.8, 17.6 Hz, 1 H), 4.23-4.16 (comp 3 H), 3.28 (dd, J = 3.2, 13.6 Hz, 1 H), 2.95 (dd, J = 10.8, 17.6 Hz, 1 H), 2.75 (dd, J = 10.0, 13.6 Hz, 1 H), 2.59 (dd, J = 4.0, 17.2 Hz, 1 H), 1.64 (m, 1 H), 1.51-1.32 (comp, 3 H), 0.92 (t, J = 7.6 Hz, 3 H).

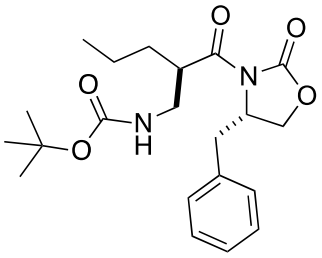

14

***tert*-Butyl R-2-((S)-4-benzyl-2-oxooxazolidine-3-carbonyl)pentylcarbamate (14). (VA-69)** Acid **8** (70 mg, 0.22 mmol), DPPA (90 mg, 70 µL, 0.328 mmol), and Et_3N (45 mg, 62 µL, 0.438 mmol) was dissolved in toluene (2.75 mL) and stirred for 1 h. The resulting solution was heated at 85 ^oC and stirred for 1 h. *tert*-BuOH (4.2 mL) was added and the solution was stirred at 85^oC for 18 h. The solvent was removed under reduced pressure and the crude material purified by flash chromatography eluting with hexanes:EtOAc (elution gradient 0% to 20% EtOAc) to yield 0.0240 g (28%) of **14** as a colorless oil: ^{1}HNMR (400 MHz, $CDCl_3$) δ 7.36-7.21 (comp, 5 H), 4.89 (brs, 1 H), 4.67 (m, 1 H), 4.18 (m, 2 H), 3.91 (m, 1 H), 3.53-3.30 (comp, 3 H), 2.77 (dd, J = 10.0, 13.2 Hz, 1 H), 1.69 (m, 1 H), 1.51-1.34 (comp, 12 H), 0.92 (t, J = 7.2 Hz, 3 H).

References

1. Homans, S.W. *Drug Discovery Today*. **2007**, *12*, 534-539.
2. Freire, E. *Drug Discovery Today.* **2008**, *13*, 869-874.
3. Loughlin, W.A.; Tyndall, J.D.A.; Glenn, M.P.; Fairlie, D.P. *Chem. Rev.* **2004**, *104*, 6085-6118.
4. Benfield, A.P.; Teresk, M.G.; Plake, H.R.; DeLorbe, J.E.; Millspaugh, L.E.; Martin, S.F. *Angew. Chem. Int. Ed.* **2006**, *45*, 6830-6835.
5. Davidson, J.P.; Lubman, O.; Rose, T.; Waksman, G.; Martin, S.F. *J. Am. Chem. Soc.* **2002**, *124*, 11058-11070.
6. Machida K.; Mayer, B.J. *Biochim. Biophys. Acta.* **2005**, *1747*, *1-25.*
7. Sawyer, T.K.; Bohacek, R.S.; Dalgarno, D.C.; Eyermann, C.J.; Kawahata, N.; Metcalf III, C.A.; Shakespeare, W.C.; Sundaramoorthi, R.; Wang, Y.; Yang, M.G. *Mini Rev. Med. Chem.*, **2002**, *2*, 475–488
8. Ward, J.M.; Gorenstein, N.M.; Tian, J.; Martin, S.F.; Post, C.B. *J. Am. Chem. Soc.* **2010**, 132, 11058-11070.
9. Tian, J. (2011) Final Report. University of Texas.
10. McKennon, M.J.; Meyers, A.I. *J. Org. Chem.* **1993**, *58*, 3568-3571.
11. Gage, J.R.; Evans, D.A. *Organic Syntheses*, **1993**, *Coll. Vol. 8*, 528.
12. Pangborn, A. B.; Giardello, M. A.; Grubbs, R. H.; Rosen, R. K.; Timmers, F. J. *Organometallics* **1996**, *15*, 1518-1520.
13. Still, W. C.; Kahn, M.; Mitra, A. *J. Org. Chem.* **1978**, *43*, 2923-2925.